Sun cubE onE (SEE): a CubeSat Mission for High-Energy Solar Observations

Berrilli F., Giovannelli L., Marcelli L., Casolino M., Curti F., De Guzman M. A., Di Tana V., Pattanaro L., Marmonti M., Terracina A., Rossi A., Berretti M., Casara L., Del Moro D., Calchetti D., Cantoresi M., Chierichini S., Giri Nair A., Konow F., Lucaferri L., Nigro G., Penza V., Pucacco G., Reda R., Scardigli S., Tombesi F., Francisco G., V., Mazzotta P., Mugatwala R., Reali E., Albertini M., Benigno N., Iovanna F., Marcanio A., Sarnari F., Natalucci S., Urban D., Illiano S., Plainaki C., Carpentiero R.

SEE mission rationale

Prioritizing CubeSat funding in heliophysics offers a great opportunity to maximize scientific return on investment in the coming decade.

The Sun CubE OnE (SEE) micro satellite stands out as a major example in heliophysics CubeSat missions due to its unique ability to simultaneously observe the Sun across multiple wavelengths, including ultraviolet (UV), X-ray, and gamma ray.

The SEE mission planning incorporates a high solar activity window during the declining phase of Solar Cycle 25. Figure illustrates the prediction for SC-25.

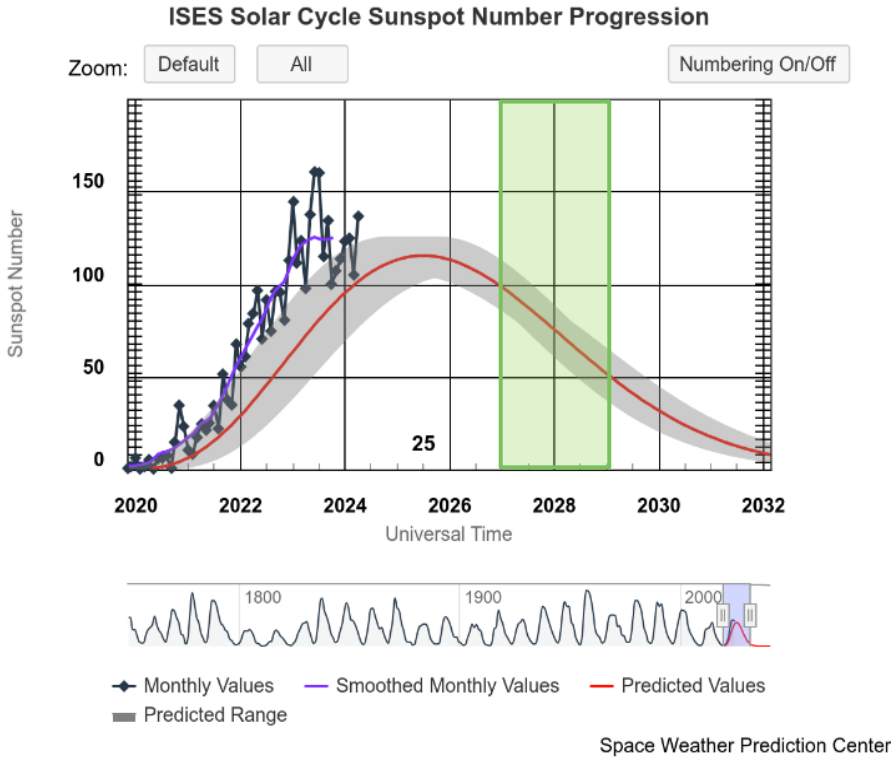

Scientific objectives

- Monitor solar flare emission from **soft-X** to **Gamma ray** energy range at very high cadence (up to 10 kHz)

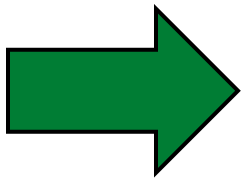

- X/γ-ray payload

- Monitor solar activity using **full disk** images in the **Mg II** at 280 nm 4 images / day to unveil **solar-terrestrial relations**

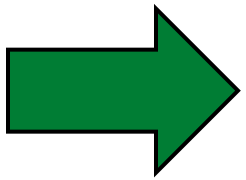

- UV imager payload

Top Level Science requirements for the UV imager and X/γ-ray payloads

TOP LEVEL SCIENCE REQUIREMENTS	
Wavelength coverage	From 279 to 281 nm
Spatial resolution	At least 4 arcsec/pixel to resolve structures
Spatial coverage (FOV)	**Full disk+50%, at least 50' x 50'**
Pointing accuracy	9' or better
Pointing stability	20 arcsec Hz or better
Temporal resolution	**One image every 6 hours**
Temporal coverage	Uninterrupted unless eclipses or contingency
Energy resolution	Spectroscopic capabilities
SNR	At least 10 considering out of band photons and straylight

TOP LEVEL SCIENCE REQUIREMENTS	
Energy coverage	**1,5 keV to 3 MeV**
Channels	4
Spatial resolution	Integrated measure
Spatial coverage	Full disk, at least 32' x 32'
Temporal resolution	**Up to 10 kHz**
Temporal coverage	**Uninterrupted unless eclipses or contingency**
Energy resolution	Spectroscopic capabilities
SNR	At least 10 based on lower energy threshold

Fast-Time Variations in X/γ-ray Fluxes during Solar Flares

Solar flares and other energetic events have been studied extensively since the first recorded observation in 1859.

Advances in observational techniques, from balloons and rockets to modern space-based telescopes, have provided unprecedented insights into the processes driving solar flares, including the acceleration of energetic particles and the heating of plasma to millions of degrees.

Understanding the fast-time variations in X-ray and gamma-ray emissions during these flares is crucial for unraveling the underlying mechanisms of particle acceleration and energy release.

Statistical studies have found that a significant percentage of large solar flares exhibit quasi-periodic pulsations (QPPs).

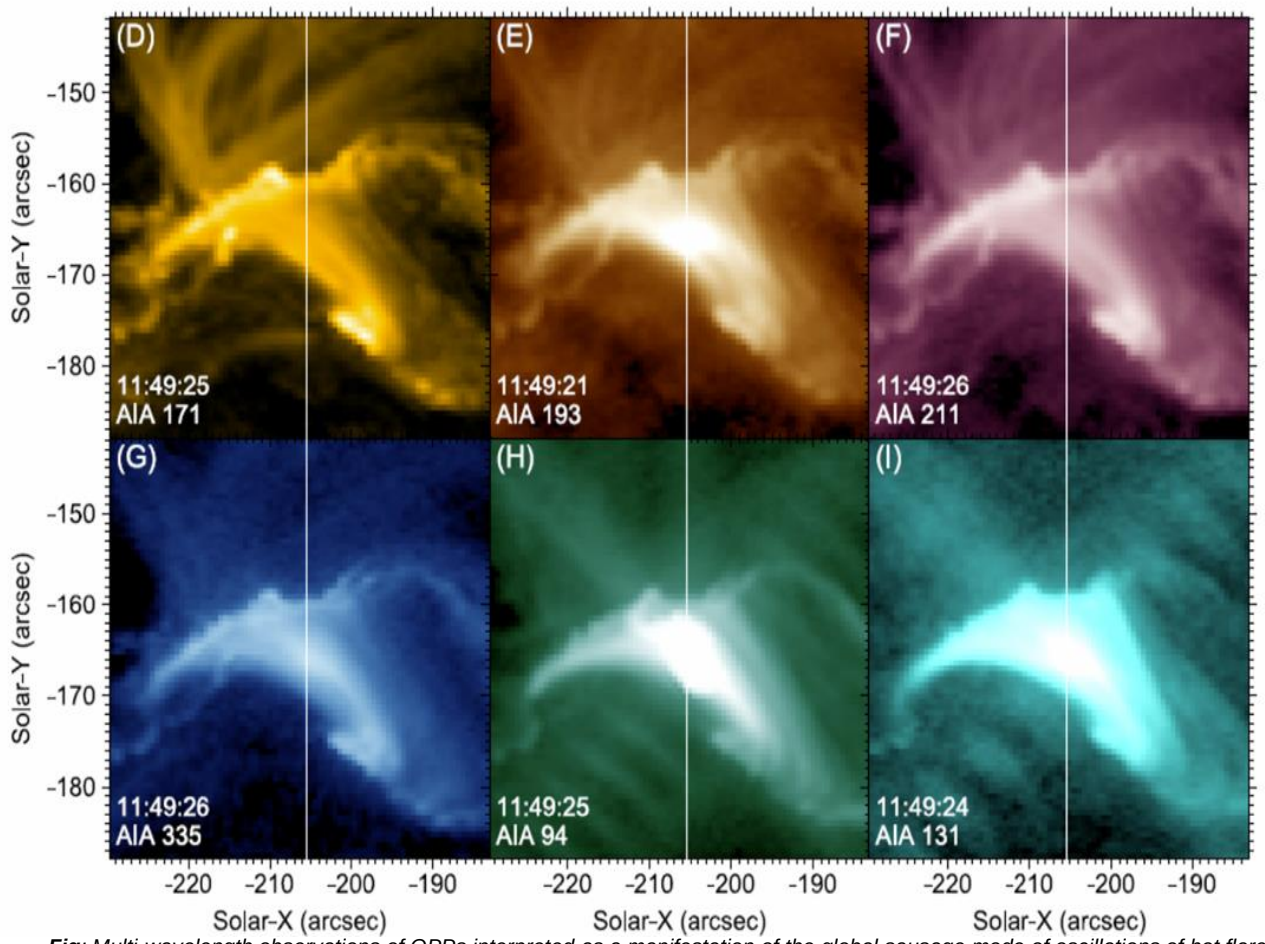

***Fig**: Multi-wavelength observations of QPPs interpreted as a manifestation of the global sausage mode of oscillations of hot flare loops. (two top panels) SDO/AIA images of the flare region in the six Fe-dominated passbands, 171 (D), 193 (E), 211 (F), 335 (G), 94 (H), and 131 (I) Å, taken around 11:49:24 UT, i.e. around the peak of an M1.6 solar flare on 2015 March 12.*

Quasi-Periodic Pulsations (QPPs) in Solar Flares

Impulsive Phase

QPPs observed during the impulsive phase of solar flares often exhibit significant variations in emission intensity, sometimes exceeding 80% modulation depth. These rapid fluctuations provide valuable insights into the particle acceleration processes occurring in the flaring region.

Decay Phase

QPPs observed during the decay phase of flares typically display characteristics of decaying quasi-harmonic signals, where the signal decay time is proportional to the oscillation period. This relationship between signal decay and oscillation period has been observed in both solar and stellar flares.

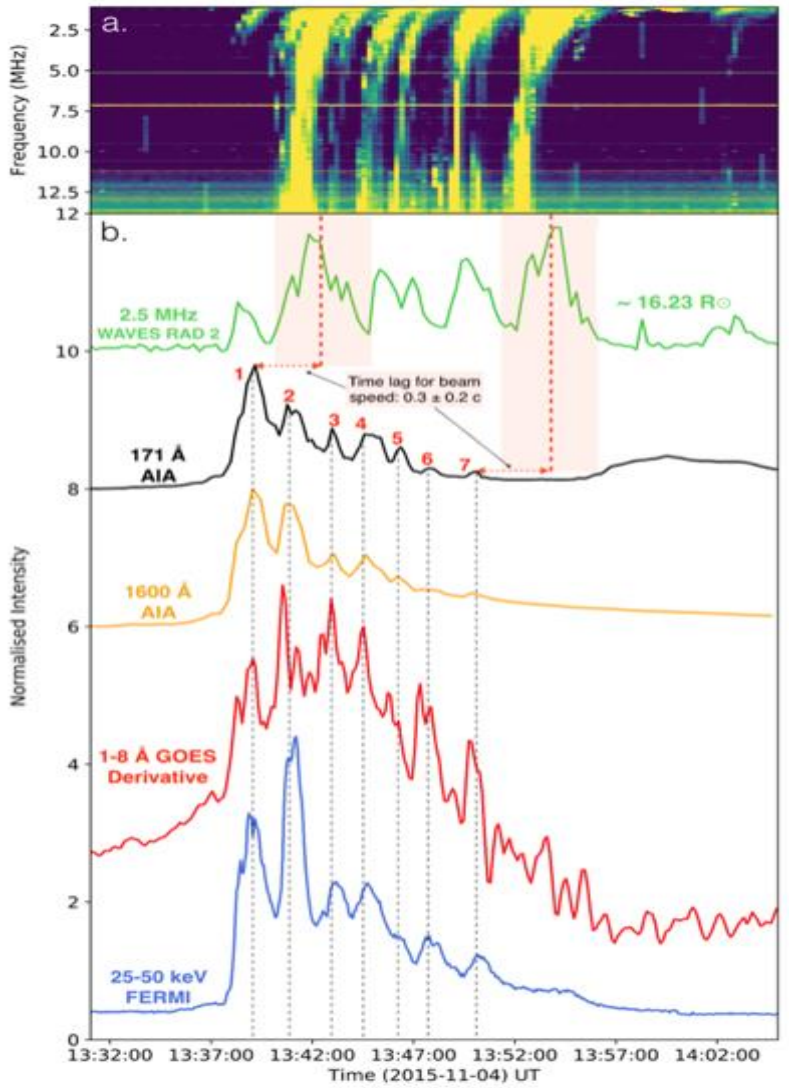

Observations of Fast-Time Variations

Subsecond Spikes

Observations have revealed the presence of rapid, subsecond spikes in hard X-ray emissions during solar flares, with some spikes as narrow as 45 milliseconds. These findings impose significant constraints on the timescales associated with nonthermal particle acceleration models.

Spectral Evolution

High-energy gamma-ray observations have revealed rapid spectral evolution of accelerated ions on timescales of approximately 30 seconds, mirroring the spectral changes observed in the lower-energy bremsstrahlung continuum.

Late-Phase Emission

An extended late-phase gamma-ray emission phenomenon has been identified, occurring subsequent to the impulsive phase and lasting for tens of minutes to tens of hours. This late-phase emission is associated with the occurrence of fast coronal mass ejections.

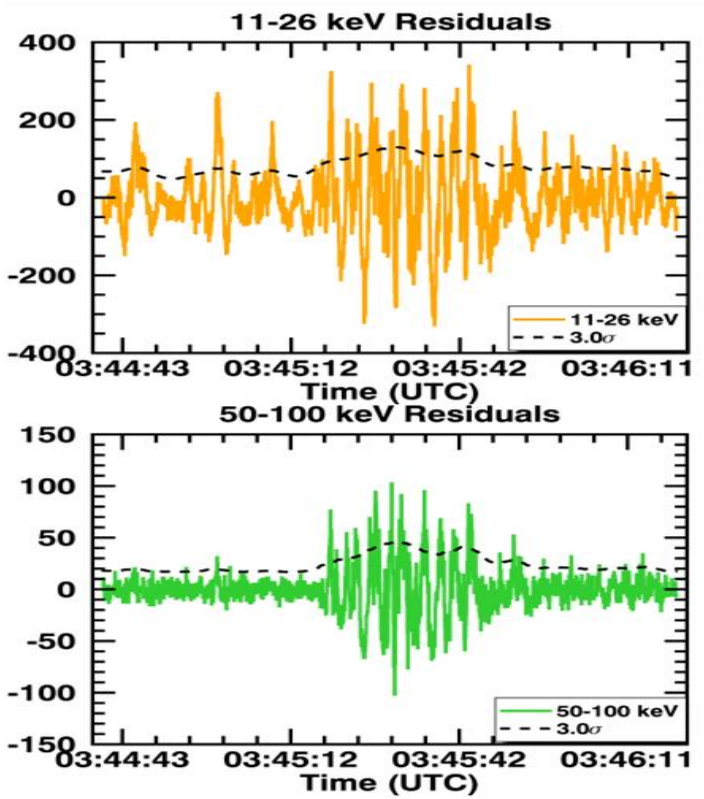

***Fig**:Subsecond fluctuations from Knuth, T., & Glesener, L. (2020)*

UV Full Disk images

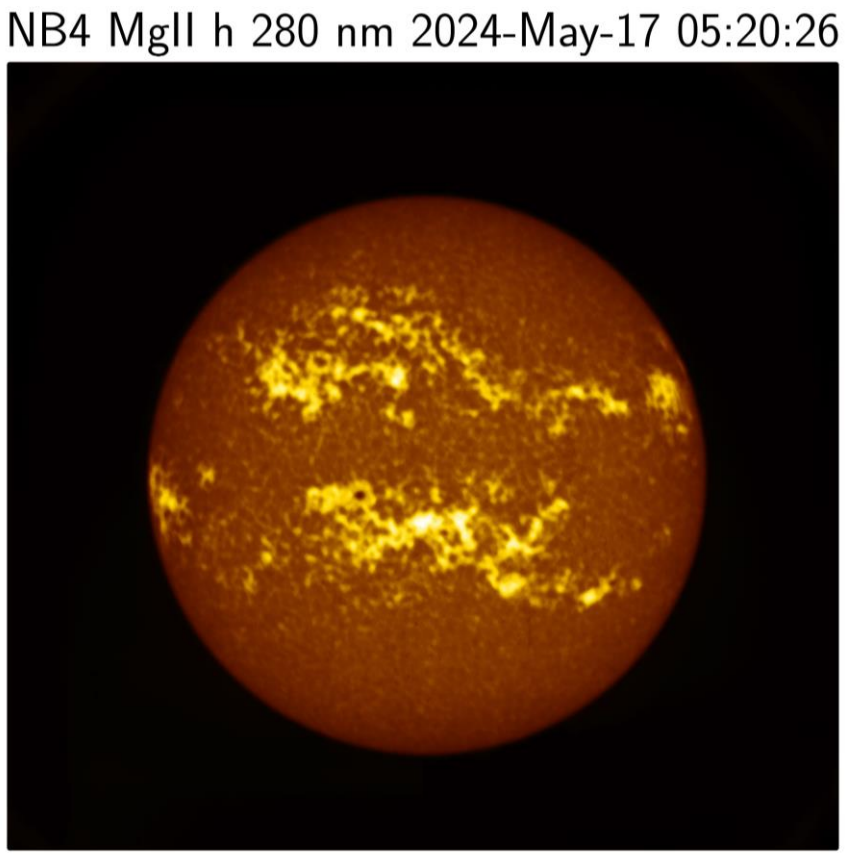

The Active region AR13664 on the Sun, during its passage during the week of May 8 – 15, 2024, erupted several X-class and M-class flares, which were associated with Coronal Mass Ejections (CMEs) during May 8 and 9. **These produced a major geomagnetic storm on May 11, 2024.**

Two of the remote sensing payloads on board Aditya-L1 (SoLEXS and HEL1OS) captured these events during May 8-9, 2024 while the two in-situ payloads (ASPEX and MAG) captured this event during May 10-11, 2024 during its passage through L1.

During those series of eruptive events, two remote sensing instruments onboard Aditya-L1, viz. the Solar UV Imaging Telescope (SUIT) and the Visible Emission Line Coronagraph (VELC) were in baking and calibration modes respectively and couldn't observe the event during May 10- 11. Both SUIT and VELC doors were opened on May 14 after the completion of the indented operations.

https://www.isro.gov.in/Aditya_L1_SUIT_VELC_Capture_SolarFury.html

Sun image in Mg II h line (NB4): Similar to NB3, NB4 shows the bright active regions on the Solar disk. The active regions signify magnetically active regions on the Sun's surface. Solar flares may originate in these active regions due to changes in magnetic fields. The Sun is moving towards solar maximum, giving rise to enhanced activity. So, there are several active regions visible around the equatorial region.

Proposed Orbits Description

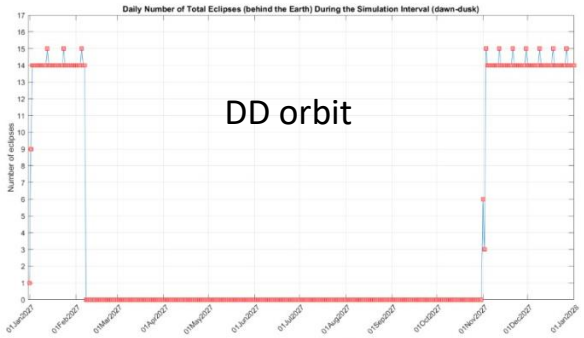

Figure 5 – Number of daily total eclipses behind the Earth throughout the simulation interval.

The duration of the eclipses during periods A and B varies (decreasing from Januar February, increasing from November to January). This is shown in Figure 6 and Figur regarding period A and B, respectively. Both figures report the total eclipse duratio every eclipse event; different markers are used for different months to highlight the tren

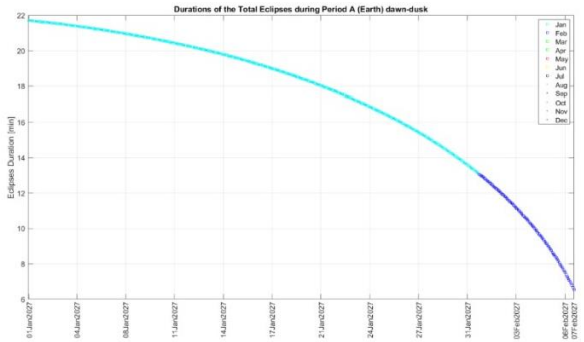

Figure 6 – Duration of each total eclipse during period A.

Table 3 – Contact with Ground Results for the DD orbit

GS	Min time [sec]	Max time [sec]	Avg time [sec]	Min n. cont. day	Max n. cont. day	Avg n. cont. day
Fucino	300.183	582.820	494.262	2	4	3.668
Malindi	301.098	581.720	493.215	1	4	2.688
Svalbard	300.726	589.021	525.746	5	13	11.436
GS-A	300.094	587.662	483.275	4	9	8.066
GS-B	300.938	583.081	494.788	2	4	3.685

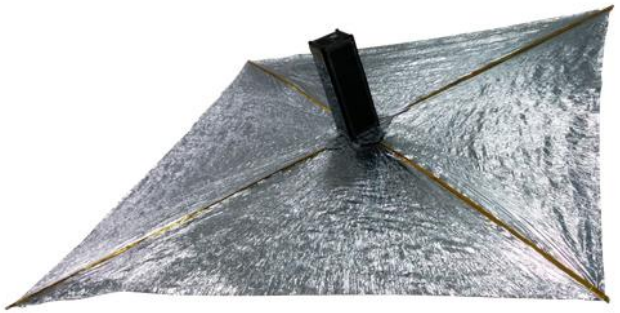

A COTS Solution for De-Orbiting: ARTICA
https://www.npcspacemind.com/cubesat-deorbiting-system/

Two orbits are considered, both of them Sun-synchronous orbits (SSO) due to the nature of the SEE program. The two orbits have the same shape, i.e., nominal altitude equal to 550 km and eccentricity equal to 0.001. The difference between the two orbit is in terms of Right Ascension of the Ascending Node (RAAN).

- Dawn-Dusk (DD) orbit – A DD orbit has the key feature of riding the terminator line, that is, it flies over a point on the Earth's surface always at the local dawn or dusk as a consequence of this, the Sun is always in the line of sight of the satellite (ideal). The selected DD has inclination equal to 97.5976 deg. The selected DD orbit is set to have the Local Time of the Ascending Node (LTAN) at 06:00:00 AM.

- 10:30 LTAN orbit – A SSO with Local Time of the Ascending Node (LTAN) set to be at 10:30 AM can be considered a generic case for Sun-Synchronous satellites.. The considered orbit has a RAAN set to be 257.781 deg and inclination equal to 97.4439 deg.

UV Mg II @280 nm Imager

The baseline optical layout selected for the telescope, is catadioptric. The choice to use a catadioptric scheme compared to a dioptric scheme allows to have a compact longitudinal size with a good image quality all over the field of view.

The optical system is composed by 5 spherical optical elements,2 spherical mirrors, and 3 spherical lenses all made in fused silica.

The choice to use a single material for all the optical elements is linked to the fact that the system is monochromatic.

Fused silica was selected as the material because it transmits very well in the UV range.

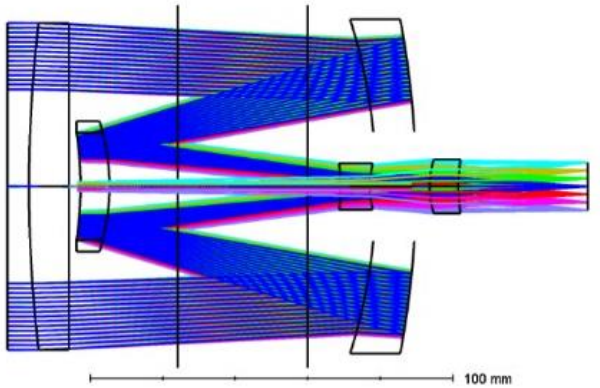

This catadioptric telescope presents two Mangin mirrors, that are lenses with the reflective surface on the rear side of the glass. The design is composed of only spherical elements, no conical or aspherical elements were used.

The compact design allows to fit the UV imager payload in less than 2U volume.

Considering only the optical parts, the dimension of the telescope is about 100 (diameter) x 160 mm.

The mass of the telescope (optical elements only) is about 600 gr.

Usually for this layout, an external baffle is not used, but two internal baffles will be integrated to avoid straylight.

System optical specifications are resumed in the following table:

Description	Value
Focal Length	690 mm
Image format	17,52 mm diagonal (14 x 10,53 mm)
Field of View (FOV)	± 0,73°
Sun Field of View	± 0,55°
Max aperture (F/N)	F/N = 7,6
Wavelength range	UV range 280 ± 2 nm
T/Number[1]	$T/N = \frac{F/N}{\sqrt{transmittance}} = 11{,}68$
Resolution	Diffraction Limit MTF = 24% @ 140lp/mm
Distortion	< 1%
Vignetting	Negligible. Considering obstruction <35
Obscuration	36 mm (physical obscuration)
Dimensions without mechanics	Diameter about 100 mm x 160 mm axial length
Interfaces	TBD

Table 4-1: Technical characteristics

X/γ-ray detectors

The X- and Gamma-ray instrument is composed on four detectors, one for the X energy range, one in the X-gamma range and two in the the gamma energy range. The current design uses CsI(Tl) or Lyso (TBD) crystals coupled with SiPMs for gamma detection or SiPM/Si-PIN for the X detection.
The X- and Gamma-ray payload is composed by:

1. Four detector elements, each composed by:
    a) Scintillator.
    b) Photodetectors: Hamamatsu SiPMs (gamma) or Si-PIN (low energy X-ray).
    c) Collimator. Tungsten or high density material.
2. Anticoincidence. A crystal/plastic anticoincidence system, surrounding all four detector elements, will be used to reject the signal coming from charged particles (mostly electrons and protons.
3. The top anticoincidence system is not present in correspondence with the entrance window of the x-ray detector.
4. Frontend/readout electronics.
5. Control Board. The board will be used for data handling, temperature control and conditioning of the SiPMs
6. Payload Computer - data processing unit (DPU) (shared with the UV-imager).
7. Power board (shared with the UV-imager).

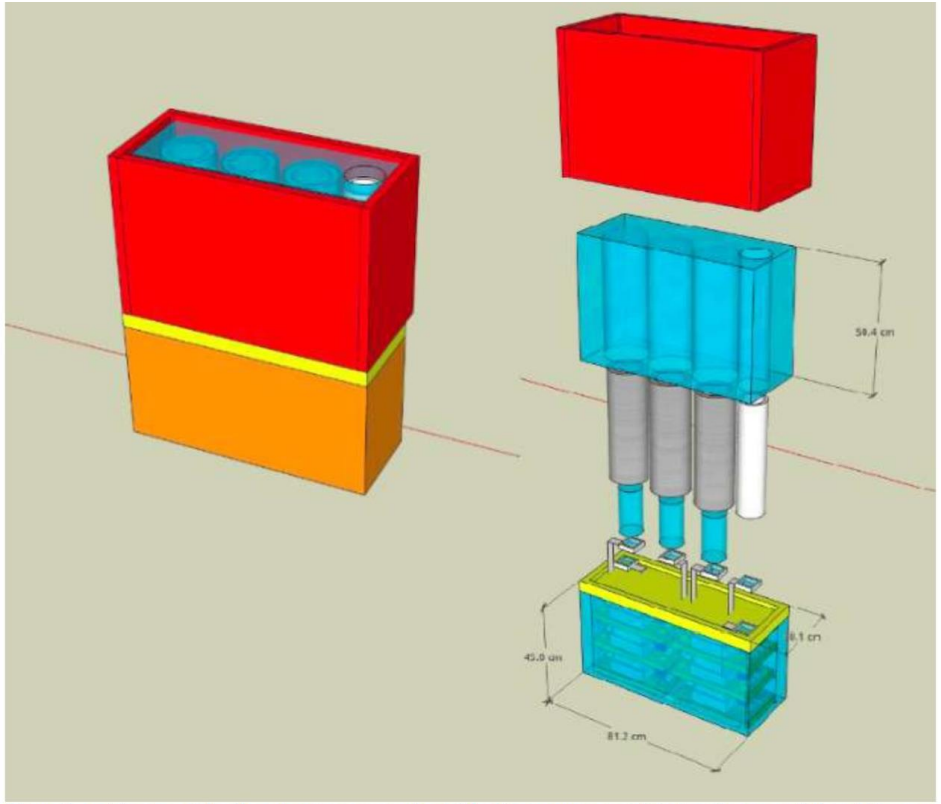

Figure 5: cad images of the X- and gamma-ray payload. The three gamma-ray detectors (in grey color) and the x-ray detector (in white color) are clearly visible. The blue box around the detector is the anticoincidence system.

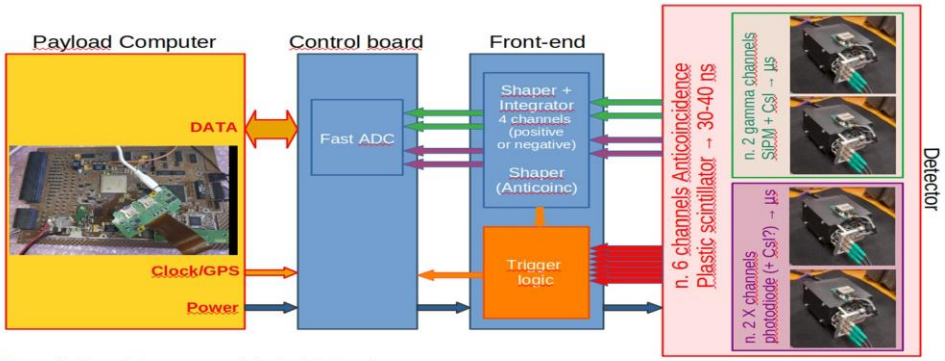

Figure 7: X- and Gamma-ray detector block scheme.

Mission profile

SEE is a 12U CubeSat (up to 24 kg) based on the ARGOTEC HAWK platform (used in LICIACube and ArgoMoon).

The HAWK platform provides: Attitude Determination and Control, Data Handling, Telemetry, Tracking & Command and Thermal Control. Most of the components already have TRL-9.

Ground Segment Definition & Operations

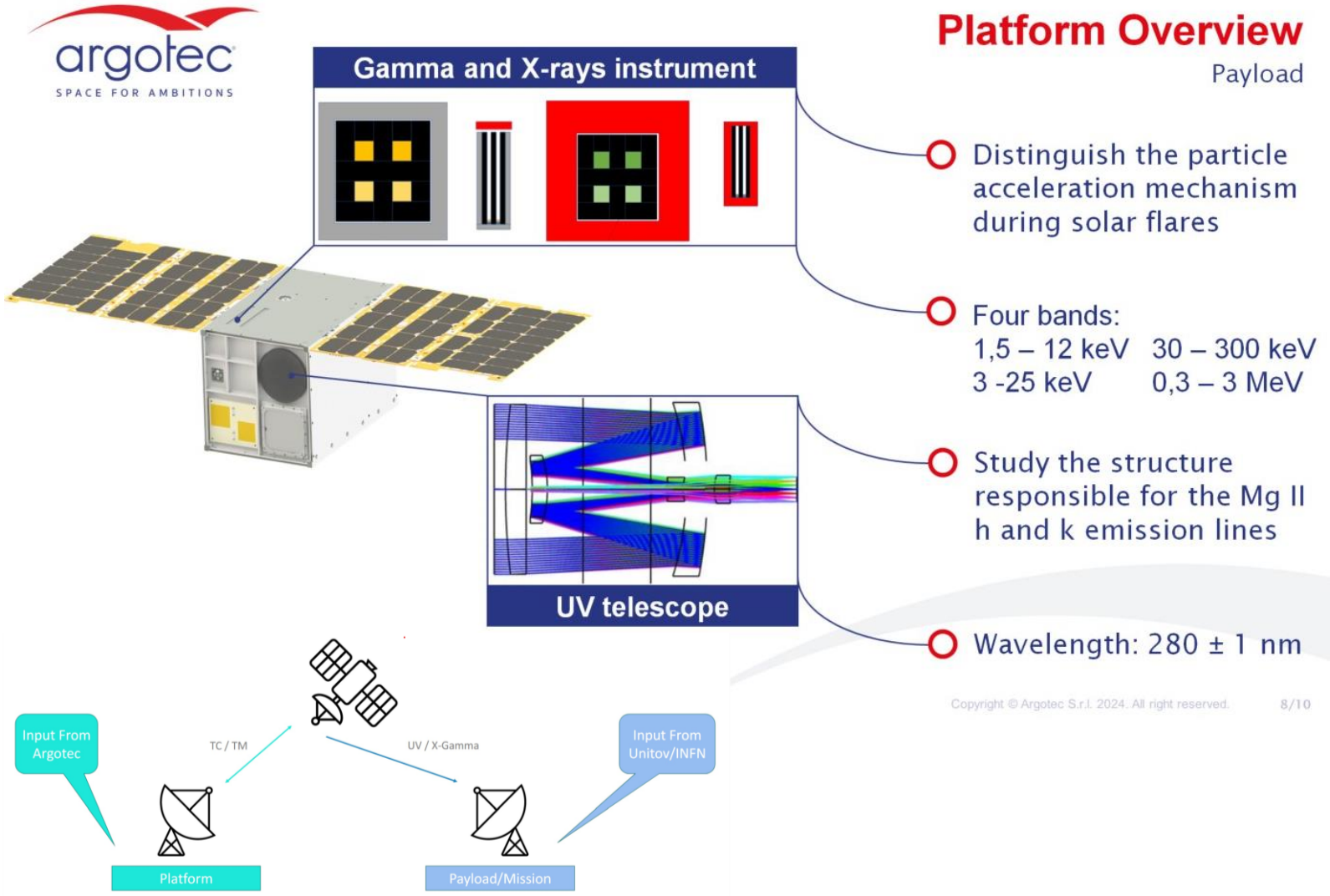

Conclusions

- **Heliophysics**
  - **UV** solar magnetic structures
  - Particle acceleration in **solar flare** events
- **Space Weather** impact: **Solar Hazard** monitoring of **solar flares from UV to HXR**
  - Critical infrastructures and Human exploration
- **Sun-Earth** connection in the **UV**
  - Ozone modulation in the stratosphere
  - Thermosphere density (satellites drag)
- ***Major technological challenges for the SEE scientific payloads:***
  - **Miniaturization** of the **UV telescope** operating at 280 nm with a suitable background rejecter filter and contamination control
  - **Miniaturization** of the X/γ-ray **detectors**